6. DESIGN OF MOTIF-BASED ALGORITHM

In the history of inspection for defects on fabric, many of the proposed methods have concentrated on non-patterned fabric defect detection. The texture background information given by this type of fabric is homogenous and seldom changed. The researchers did not need to consider the relationship between designed pattern and defects. Besides, there are over seventy common defects on this type of fabric. The work in dealing with such a large amount of defects for detection and classification has been the focus in the past twenty years. Out of the many methods, image subtraction method and hash function method, are predominant in usage for fault identification in patterned fabrics. As both the methods' performance degrades in the presence of noise, research for other suitable technique is an ongoing process.

Ngan *et al.* (2008) proposed a generalized motif-based method for defect detection in patterned fabrics. This system provides several advantages to patterned fabric defect detection process and is listed below.

(i) Presents a generalized algorithm that can deal with 16 out of 17 patterned groups without any modification

(ii) No ground truth or supervisory learning procedure is required

(iii) It is invariant to slight distortion, quantization errors and misalignment of lattices

(iv) Produced a high defect detection success rate of 93.32%

In order to further improve the above system, the third phase of the study proposes a motif-based technique that includes two steps to the Ngan model. The first step performs an automatic extraction of lattice and motifs, while the second step considers both circular shift operation and spatial relationship between pixels to improve the efficiency of fault detection in patterned fabrics. The steps involved in the proposed motif-based defect detection system are given in Figure 6.1. This chapter presents description on each of these steps.

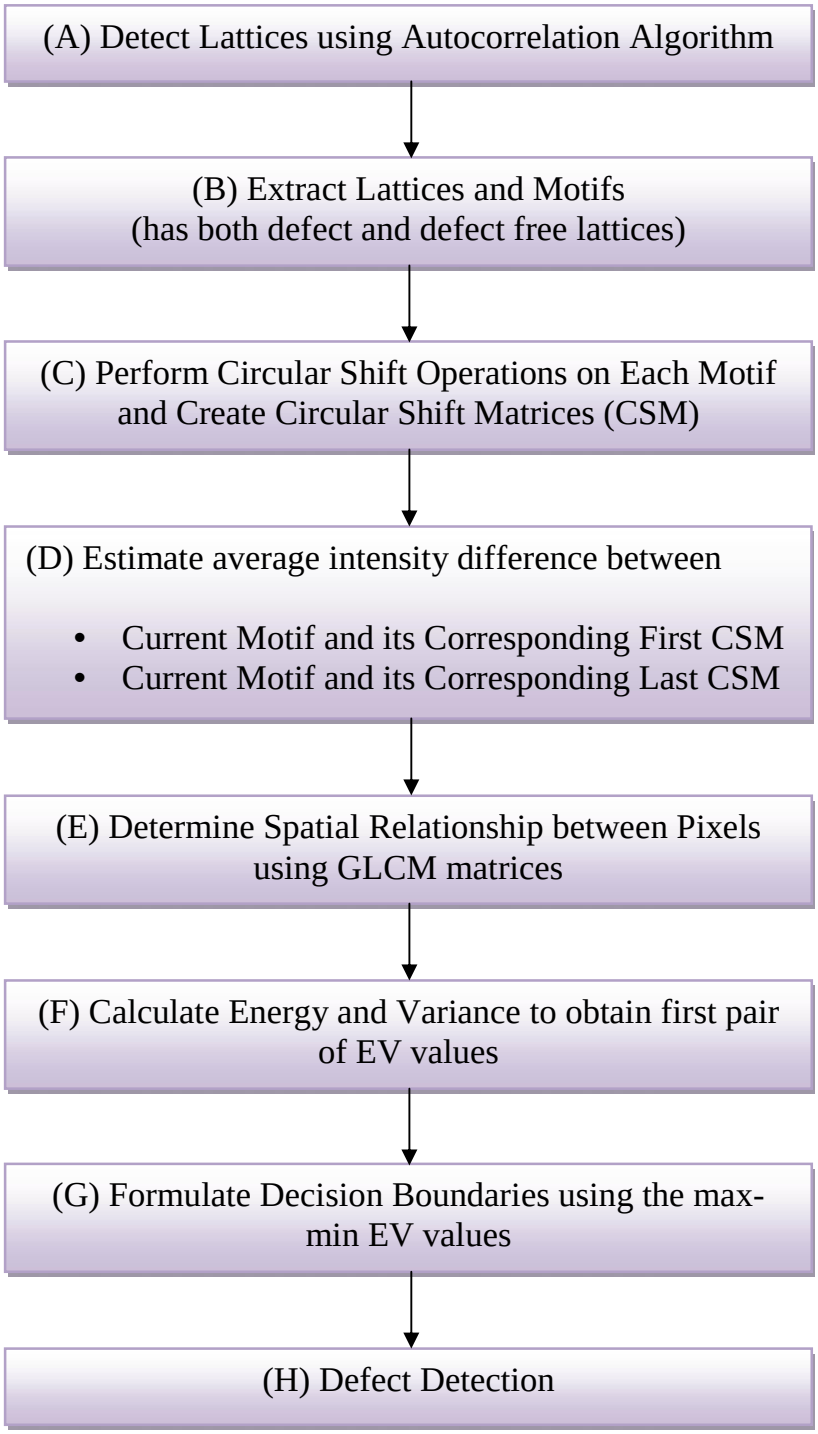

Figure 6.1 : Proposed Motif-Based Defect Detection System

Let a w × t patterned texture, F = [f(a,b)] and a p × q lattice, L = [f(a,b)], be expressed as 2D arrays of real values where each element at f(a,b) ∈ [0, 1] represents the intensity level of a pixel of a patterned texture and a lattice, respectively. A lattice is defined as L = [f(a,b)] and a defective lattice, $\overline{L}$, is

defined as $\bar{L}$ = L + P = [$\bar{f}$ (a,b)] where $\bar{f}$ (a,b) = f(a,b) + ε (a, b) and P = [ε(a, b)] is a p ×q matrix that represents additive defects and ε(a, b) ∈ R, $0 \leq \bar{f}(a,b) \leq 1$, $1 \leq a \leq p$ and $1 \leq b \leq q$. A motif is defined as M=[f(c,d)] and a defective motif, M, is defined as M=M+P =[$\bar{f}$ (c,d)] where $\bar{f}$ (c,d)= f(c,d) + e(c, d) and P = [e(c, d)] is an m × n matrix that represents additive defects and e(c, d) ∈ R, $0 \leq \bar{f}(c,d) \leq 1$, $1 \leq c \leq m$ and $1 \leq d \leq n$. As mentioned earlier, motif is a fundamental unit of a lattice, from which a lattice can be regenerated completely by replicating the motif through isometric operations.

Given any two m × n motifs, $M^s = [f^s(c, d)]$ and $M^r = [f^r(c, d)]$ from lattice L, a k-norm metric between two motifs is defined using Equation (6.1).

$$u^{s,r} = \left\| M^s - M^r \right\|_k / N = \left(\sum_{c=1}^{m} \sum_{d=1}^{n} \left| f^s(c,d) - f^r(c,d) \right|^k \right)^{1/k} / N \quad (6.1)$$

where N = m . n. If $M^s = M^r$, then $u^{s,r} = 0$, else $0 < us,r \leq 1$. k is set to 1 for k-norm metric as it represents the simplest case. By basic combinatorics, the total number of 1-norm metric for $u^{s,r}$ in one lattice is C_2^n, where n is the total number of motifs in a lattice. As there is only one motif in the p1 group, it does not fall within the definition of 1-norm metric and therefore, cannot be dealt with by this method.

6.1. LATTICE EXTRACTION

The most important task in repeated pattern analysis is the problem of extracting lattices correctly. Several works has been proposed for this purpose which can be grouped into three main categories, namely, feature based techniques, autocorrelation (Lin *et al.*, 1997) based techniques and texture based techniques. All the methods have the advantage of detecting small repeated patterns from a large image and can also group elements that have surface deformations like folds. When compared to autocorrelation method, the other two

methods have the drawback of required distinct corner / edge / contour definition and the assumption that a single periodic pattern occupies a large portion of the image, limiting the approach to analysis of patterns that have already been segmented in some other way. In this study, the autocorrelation method proposed by Liu *et al.* (2004) is used and is described in the following section. This method consists of the following steps.

(i) Peak Detection using Region of Dominance
(ii) Determine the Shortest, Independent Translation Vectors
(iii) Symmetry Group Classification

6.1.1. Peak Detection

This step extracts a set of linearly independent vectors that describe the translational symmetry of the pattern by searching for peaks in the autocorrelation surface of the pattern. It is an important task to find a proper set of peaks in an autocorrelation surface of a periodic pattern. It is based on the assumption that absolute height of a peak is not as important as the size of its region of dominance, defined as the largest circle centered on the candidate peak such that no higher peaks are contained in the circle.

A peak with a low height, but located far from any larger neighbors, is much more perceptually important than a high peak that is close to an even higher one. A list of peaks in decreasing order of dominance can be computed using a simple N^2 algorithm, where N is the number of candidate peaks to be considered. These initial peaks P_1, P_2, ..., P_N are computed using non-maximum suppression over a sliding M x M window, where M is set to 5 in experiments and is selected based on the scale of the pattern to yield fewer initial candidates.

The method first sorts candidate peaks in descending order of peak height (N*LOGN) to yield a list Q_1, Q_2, ..., Q_N. Next, for each Q_j, the distance to each Q_i, $1 \leq i < j$ that comes before it in the list is computed and is denoted as the minimum distance, D_i. This is an order N^2 process. Finally, the list of peaks is sorted again in

descending order of D_i, which is the minimum distance to a higher peak. The peaks are now arranged in decreasing order of dominance. This approach to peak detection has several advantages.

(i) works well on a diverse set of autocorrelation images
(ii) generalizes readily to any dimension
(iii) is potentially useful in other vision contexts where multiple peaks must be detected within accumulated noisy data

6.1.2. Determine the Shortest, Independent Translation Vectors

After obtaining the set of candidate lattice points, extracted as dominant peaks in the autocorrelation surface, the next step finds the shortest linearly independent translation vectors that generate the lattice. For wallpaper patterns two vectors are required and the angle between them must be between 60 and 90 degrees (Schattschneider, 1978). For this purpose, Hough transformation approach is used to find the two shortest translation vectors that best explain the majority of the point data.

6.1.3. Symmetry Group Classification (Motif)

A symmetry g of a 2D periodic pattern P is a distance preserving mapping (translation, rotation, reflection or composition) that maps every pixel in the pattern to a pixel of the same grey-value or color such that $g : R^2 \times I \Rightarrow R^2 \times I$ and $g(P) = P$ where I can either be gray values in the range of [0, 255]. The set of all symmetry transformations of P comprises the pattern's symmetry group. Mathematically, symmetry groups are defined only for periodic patterns of infinite extent. Generally, a periodic pattern bounded within a finite image area is analyzed and the concept of symmetry group G of P to mean G is used as the symmetry group of an infinite periodic pattern for which P is a finite patch.

A periodic pattern extended in two linearly independent directions to cover the 2D plane is known as a wallpaper pattern. The two smallest linearly independent translation vectors T1 and T2 in the pattern's symmetry group are

generators for the underlying lattice structure of the pattern. That is, the orbit of any point under these two translations forms the vertices of a lattice. The lattice divides the plane into identical parallelogram-shaped sub-images, called lattice units or tiles.

The symmetry group of a wallpaper pattern has to be one of only 17 distinct wallpaper groups. An accessible proof of this fact was presented by Schwarzenberger (1974). The unit lattice shape for each of the 17 wallpaper groups, with the geometric configuration of translation generators, rotation, reflection and glide-reflection symmetries superimposed for each group was presented in Chapter 1, Figure 1.5. Each unit lattice is also labeled using the crystallographic notation (Henry and Lonsdale, 1969) consisting of four symbols that identify the conventionally chosen lattice unit, the highest order of rotation, and other fundamental symmetries.

A lattice unit is typically chosen with centers of highest order of rotation at the vertices. In two cases (cm; cmm) a lattice unit is chosen where reflection axes are normal to one or both sides of the lattice unit. The correct pattern classification can be performed after verifying the existence of only a small set of symmetries, specifically four rotations of 180, 120, 90 and 60 degrees, and four reflections along axes parallel to either unit lattice parallelogram boundaries T1 and T2 or diagonals D1 and D2. The algorithm used for classifying the symmetry group of a wall paper pattern is given below.

1. Find the pattern lattice: Compute the underlying pattern lattice

2. Estimate a median tile and noise model: Cut out a set of tile-shaped regions from the input pattern using the overlaid lattice. Choose one of these as a reference tile and register it with all other tiles in the set using a Sum of Squared Difference (SSD) measure. This yields a set of corresponding intensity measurements for each pixel in the tile. Compute an estimate of the noise-free tile by assigning each pixel the median value of its set of intensity measurements. Also form an estimate of the pixel noise level by computing the

standard deviation σ of the residuals between all pixels and their corresponding median tile values. This noise model assumes that a pattern tile is generated by taking the median tile and applying independent Gaussian noise at each pixel, with mean 0 and standard deviation σ.

3. Test symmetries: Test for the existence of rotation and reflection symmetries in the pattern. Eight symmetries are tested for wallpaper groups (Table 6.1). The steps taken for each symmetry are:

   - apply the symmetry to the original image (e.g. rotate the image by 180 degrees) to obtain a transformed image I'.
   - correlate the median tile with image I' at all lags to get a rough registration map.
   - start at the point with highest correlation value and register the median tile with I' by finding a small translation that minimizes SSD registration error.
   - at the position of best registration, compute the trimmed normalized residual error using Equation (6.2).

$$d = \sum_{k=1}^{N'} e_k = \sum_{k=1}^{N'} \frac{(m_k - i_k)^2}{\sigma^2} \qquad (6.2)$$

     where N is the total number of pixels in the tile, N' = (1 - b)N is a smaller number of pixels as determined by d, the trim rate, which is the percentage of pixels to be discarded from the end of the e_k error sequence when e_k is sorted in ascending order (the higher on the queue the “noisier" the pixels), m_k, i_k are corresponding pixel intensity values of the median tile and image I', respectively, and σ is the standard deviation of the pixel noise model.

   - repeat the computation of trimmed normalized residual errors d_i at neighboring lattice points and keep the error value d_{med} = median$\{d_i\}$ which is the median among all computed errors. The idea behind this step is to guard against accepting accidental good alignments between the median tile

and transformed image as evidence of the existence of symmetry. A proper symmetry must also preserve the original image's lattice structure.

- if it is assumed that pixel values are corrupted by independent Gaussian noise with mean 0 and standard deviation σ, then d_{med} should obey a $\chi 2(N')$ distribution with N' degrees of freedom. Evaluate whether the tested symmetry exists by comparing d_{med} to a threshold T where $\int_0^T \chi^2_{N'}(x)dx = 0.99$. The symmetry is said to exist if $d_{med} < T$, otherwise not. Moreover, $T \approx N'$, for large N' and thus an approximate test for symmetry is whether $d_{med}=N' < 1.0$.

- as an additional step when a reflection symmetry is found to exist, decide if it is a glide reflection or not by examining the offset of the location of best registration between the median tile and the transformed image I' to the location where the center of the original reference tile is mapped to in I'. This offset should be roughly an integer multiple of one of the lattice vectors if we have pure reflection, otherwise it falls roughly halfway between integer multiples, and is labeled as a glide reflection.

4. Classify the symmetry group: validate the symmetry test results against the symmetries listed in Table 6.1 to classify the symmetry group of the pattern.

TABLE 6.1

WALLPAPER GROUP CLASSIFICATION

	p1	**p2**	**pm**	**pg**	**cm**	**pmm**	**pmg**	**pgg**	**cmm**	**p4**	**p4m**	**p4g**	**p3**	**p3m1**	**p31m**	**p6**	**p6m**
180		Y				Y	Y	Y	Y	Y	Y	Y				Y	Y
120													Y	Y	Y	Y	Y
90										Y	Y	Y					
60																Y	Y
T1			Y	Y(g)		Y	Y(g)	Y(g)			Y	Y(g)			Y		Y
T2						Y	Y	Y(g)			Y	Y(g)			Y		Y
D2					Y				Y		Y	Y		Y	Y		Y
D2									Y		Y	Y					Y
DOF	N	N/2	N/2	N/2	N/2	N/4	N/4	N/4	N/4	N/4	N/8	N/8	N.3	N/6	N/6	N/6	N/12

6.2. MOTIF EXTRACTION

When translational symmetry is determined for a periodic pattern, it fixes the size, shape and orientation of the unit lattice but leaves open the question of where the unit lattice is located in the image. Figures 6.2a and b shows an automatically extracted lattice and the tile that it carves out, on an patterned fabric image. The tile is not a good representation of the pattern motif. Figure 6.2c and d show the lattice position in terms of one of the three most-symmetric motifs found for the oriental rug image. The latter was generated automatically by the algorithm discussed in the previous section, which analyzes pattern symmetry based on knowledge of the 17 wallpaper groups.

The pattern fragment on the tile appears non-intuitive to a human observer, even though it is mathematically correct. If the goal is to tile the plane, any parallelogram of the same size and shape produces an equally good lattice unit. However, from a perception point of view, some parallelograms produce tiles that are much better descriptors of the underlying symmetry of the overall pattern than others. For example, if the whole pattern has reflection symmetries, it is desirable to have the lattice unit in isolation to also exhibit this reflection symmetry.

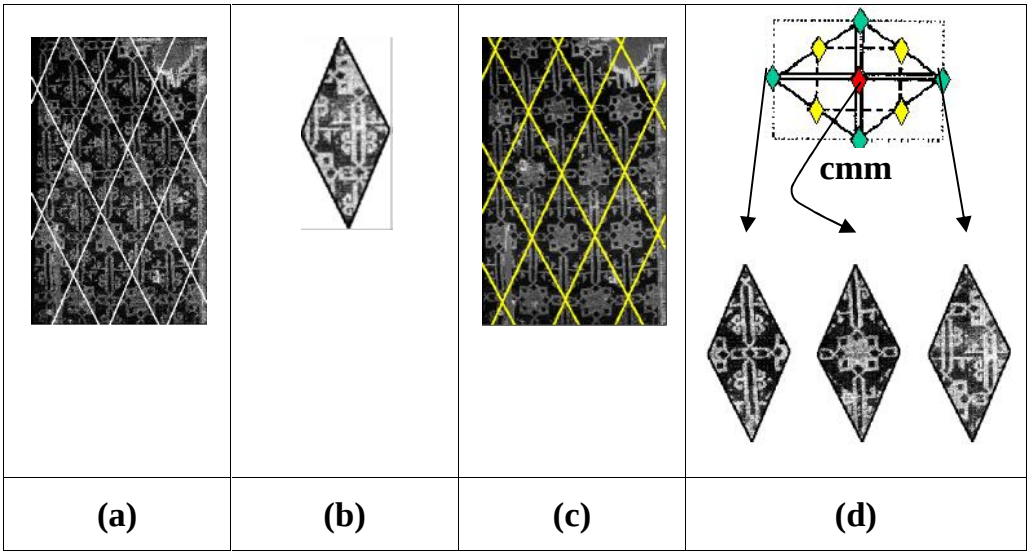

Figure 6.2 : Motif Extraction Example

The motif is defined as a representative tile of a periodic pattern. Choosing a good motif should help to see what the pattern looks like, from a single tile. This is related to the problem of figure-ground separation. It is desirable to find a motif that is centered on the foreground “figure”, rather than having the figure split into two or more pieces on opposite edges of the tile.

According to Leyton (1992), it is known that the human perceptual system often has a preference for symmetric figures. As the most representative motif is the one that is most symmetrical, the solution for generating motifs is to align the motif center with the center of the highest-order rotation in the pattern. This is the lattice point with the largest stabilizer group (Liu, 1990).

Candidate motifs can then be determined systematically by enumerating each distinct center point of the highest-order rotation. Two rotation centers are distinct if they lie in different orbits of the symmetry group, that is, if one cannot be mapped into the other by applying any translation, rotation, reflection or glide-reflection symmetry within the symmetry group.

6.3. CREATION OF CIRCULAR SHIFT MATRICES

Given any m x n motif (Equation 6.3), a circular shift operation H of a matrix produces m x n new motifs such that $M_{ij} = H[M]$ is defined using Equation (6.4).

$$M = \left[f(c,d) \right] = \begin{bmatrix} f(1,1) & f(1,2) & \cdots & f(1,n) \\ f(2,1) & f(2,2) & \cdots & f(2,n) \\ \vdots & \vdots & & \vdots \\ f(m,1) & f(m,2) & \cdots & f(m,n) \end{bmatrix} \qquad (6.3)$$

$$M_{11} = \begin{bmatrix} f(1,1) & f(1,2) & \cdots & f(1,n) \\ f(2,1) & f(2,2) & \cdots & f(2,n) \\ \vdots & \vdots & & \vdots \\ f(m,1) & f(m,2) & \cdots & f(m,n) \end{bmatrix},$$

$$M_{12} = \begin{bmatrix} f(1,2) & \cdots & f(1,2) & f(1,1) \\ f(2,2) & \cdots & f(2,n) & f(2,1) \\ \vdots & \vdots & & \vdots \\ f(m,2) & \cdots & f(m,n) & f(m,1) \end{bmatrix}, \quad \ldots,$$

$$M_{1n} = \begin{bmatrix} f(1,n) & f(1,1) & \cdots & f(1,n-1) \\ f(2,n) & f(2,1) & \cdots & f(2,n-1) \\ \vdots & \vdots & & \vdots \\ f(m,n) & f(m,1) & \cdots & f(m,n-1) \end{bmatrix},$$

$$M_{21} = \begin{bmatrix} f(2,1) & f(2,2) & \cdots & f(2,n) \\ \vdots & \vdots & & \vdots \\ f(m,1) & f(m,2) & \cdots & f(m,n) \\ f(1,1) & f(1,2) & \cdots & f(1,n) \end{bmatrix},$$

$$M_{22} = \begin{bmatrix} f(2,2) & \cdots & f(2,n) & f(2,1) \\ \vdots & \vdots & & \vdots \\ f(m,2) & \cdots & f(m,n) & f(m,1) \\ f(1,2) & \cdots & f(1,n) & f(1,1) \end{bmatrix}, \ldots,$$

$$M_{2n} = \begin{bmatrix} f(2,n) & f(2,1) & \cdots & f(2,n-1) \\ \vdots & \vdots & & \vdots \\ f(m,n) & f(m,1) & \cdots & f(m,n-1) \\ f(1,n) & f(1,1) & \cdots & f(1,n-1) \end{bmatrix}, \ldots,$$

$$M_{m1} = \begin{bmatrix} f(m,1) & f(m,2) & \cdots & f(m,n) \\ f(1,1) & f(1,2) & \cdots & f(1,n) \\ \vdots & \vdots & & \vdots \\ f(m-1,1) & f(m-1,2) & \cdots & f(m-1,n) \end{bmatrix},$$

$$M_{m2} = \begin{bmatrix} f(m,2) & \cdots & f(m,n) & f(m,1) \\ f(1,2) & \cdots & f(1,n) & f(1,1) \\ \vdots & & \vdots & \vdots \\ f(m-1,2) & \cdots & f(m-1,1) & f(m-1,1) \end{bmatrix}, \ldots,$$

$$M_{mn} = \begin{bmatrix} f(m,n) & f(m,1) & \cdots & f(m,n-1) \\ f(1,n) & f(1,1) & \cdots & f(1,n-1) \\ \vdots & \vdots & & \vdots \\ f(m-1,n) & f(m-1,1) & \cdots & f(m-1,n-1) \end{bmatrix} \qquad (6.4)$$

Given M^s, M_{ij}^r where M_{ij}^r is one of the circular shift matrices, the 1-norm metric between them is defined as $u_{ij}^{s,r} = \| M^s - M_{ij}^r \|_1/N$. Figure 6.3 depicts circular matrices, M_{ij}^r, of a motif. $u_{ij}^{s,r} > 0$ for any two motifs M^s, M_{ij}^r where $M^s \neq M_{ij}^r$.

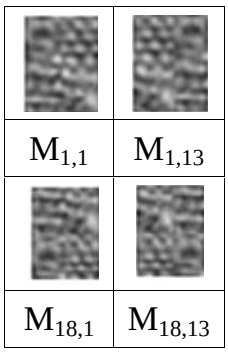

Figure 6.3 : Motif $M_{1,1}$ of size 37 × 27 and three of its Circular Shift Matrices

The process of circular shift operation let every pixel in one motif manipulate with every pixel in another motif. There is no need to have precise aligned motif on another one as in the usual image difference method. As the input lattices would have slight distortion and misalignment errors, the definition of the circular shift operation will break the spatial relationships of pixels and prevent the effect of those errors to occur.

An average intensity difference (equivalent to 1-norm metric) between motif and its corresponding first circular shift matrices is calculated. Similarly, the average intensity difference between the current motif and its corresponding last circular shift matrix is calculated.

6.4. SPATIAL RELATIONSHIPS

The Gray Level Co-occurrence Matrix (GLCM) and associated texture feature calculations are image analysis techniques. Given an motif image composed of pixel each with an intensity (a specific gray level), the GLCM is a tabulation of how often different combinations of gray levels co-occur in an image or image section. Texture feature calculations use the contents of the GLCM to give a measure of the variation in intensity (image texture) at the pixel of interest. First, the GLCM is created, which will be a square matrix N x N in size. The matrix is created as follows:

1. Let s be the sample under consideration for the calculation.

2. Let W be the set of samples surrounding sample s which fall within a window centered upon sample s of the size specified under Window Size.

3. Considering only the samples in the set W, define each element i,j of the GLCM as the number of times two samples of intensities i and j occur in specified Spatial relationship (where i and j are intensities between 0 and Number of levels-1). The sum of all the elements i, j of the GLCM will be the total number of times the specified spatial relationship occurs in W.

4. Make the GLCM symmetric:

    1. Make a transposed copy of the GLCM

    2. Add this copy to the GLCM itself

6.5. AMPLIFICATION OF DEFECT INFORMATION USING ENERGY OF MOVING SUBTRACTION

Given any two m x n motifs $M^s = [f^s(c, d)]$ and $M^r = [f^r(c, d)]$ from lattice L, there exists a set of circular shift motifs, M_{ij}^r and m . n 1-norm metrics $\left\{u_{11}^{s,r}, u_{12}^{s,r}, ..., u_{mn}^{s,r}\right\}$ for M^s , M^r and an energy of moving subtraction between M^s and M_{ij}^r is defined as $K_{s,r} = \left(\sum_{i=1}^{m} \sum_{j=1}^{n} \| M^s - M_{ij}^r \| / N^2 \right)$ where $0 \le K_{s,r} \le 1$.

Given any two m × n defect-free motifs $M^s = [f^s(c, d)]$ and $M^r = [f^r(c, d)]$ in lattice L, their corresponding defective motifs can be defined as $\overline{M}^s = M^s + P^s = [\bar{f}^s(c,d)]$ and $\overline{M}^r = M^r + P^r = [\bar{f}^r(c,d)]$, where $[\bar{f}^s(c,d)] = f^s(c, d) + e^s(c, d)$, $[\bar{f}^r(c,d)] = f^r(c,d) + e^r(c, d)$ for some additive defects $e^s(c, d), e^r(c, d) \in R$. Their circular shift motifs are defined as

The 1-norm metric between the two motifs can take three forms as follows:

(i) $\bar{u}_{ij}^{s,r} = \left\| \overline{M}^s - \overline{M}_{ij}^r \right\|_1 / N$

(ii) $\bar{u}_{ij}^{s,r} = \left\| M^s - \overline{M}_{ij}^r \right\|_1 / N$

(iii) $\bar{u}_{ij}^{s,r} = \left\| \overline{M}^s - M_{ij}^r \right\|_1 / N$

where $\overline{M}^s$, $\overline{M}^r$ are defective motifs and M^s ,M^r are defect-free motifs. It can be defined that:

(1) The range of 1-norm metric $\bar{u}_{ij}^{s,r}$ between a defective and a defect-free motif of a lattice L is $u_{ij}^{s,r} - |e| \leq \bar{u}_{ij}^{s,r} \leq u_{ij}^{s,r} + |e|$ where $u_{ij}^{s,r}$ is 1-norm metric between two defect-free motifs.

(2) For $e \neq 0$, there exists a tolerance of quantization errors, σ_{ij}, for the 1-norm metric. For $\sigma_{ij} \geq 0$, the difference in 1-norm metric between defect-free and defective motifs of a lattice is in the range $0 \leq \sigma_{ij} \leq |\bar{u}_{ij}^{s,r} - u_{ij}^{s,r}| \leq |e|$, where $|e| = \max\{|e^{s,r}|, |e^{s}|, |e^{r}|\} = |e^{s,r}|, e^{s,r}, e^{s}, e^{r} \in R$ because $|e_{s,r}(c, d)|=2$ when $e^{s}(c,d) = 1$ and $e_{ij}^{r}(c, d) = -1$ or $e^{s}(c, d) = -1$ and $e_{ij}^{r}(c,d) = 1$.

Given any m x n lattice L, with energy of moving subtraction of $\overline{K}_{s,r}$ from defective motif(s) and energy of moving subtraction of $K_{s,r}$ from defect-free motifs, the difference in energies of moving subtraction between defect-free motif and defective motif is in the range $0 \leq |\overline{K}_{s,r} - K_{s,r}| \leq m \,.\, n \,.\, |e|$ where $e \in R$ is the defect values and $|e| = |e^{s,r}|$, $e^{s,r} \in R$.

Given any m x n defect-free motif and defective motif(s) of lattice L, the defective information $e \in R$ of the difference in the calculation of energy of moving subtraction as a range is amplified for defective motifs $\overline{M}^{s}$ and $\overline{M}^{r}$ if and only if $m \,.\, n \,.\, \sigma \geq \delta$ where $\sigma = \max_{ij}\{\sigma_{ij}\}$ is a tolerance of quantization errors for the 1-norm metric, $\delta \geq 0$, is a tolerance in energy of moving subtraction and defect values $|e| = |e^{s,r}|$, $e^{s,r} \in R$, provided that:

(1) The difference in 1-norm metrics, $u_{ij}^{s,r}$ and $\bar{u}_{ij}^{s,r}$, as a range is $0 \leq \sigma_{ij} \leq |\bar{u}_{ij}^{s,r} - u_{ij}^{s,r}| \leq |e|$ where $\sigma_{ij} \geq 0$.

(2) The difference in energies of moving subtraction, $K_{s,r}$ and $\overline{K}_{s,r}$, as a range is $0 \le \delta \le |\overline{K}_{s,r} - K_{s,r}| \le m \,.\, n \,.\, |e|$ where $\delta \ge 0$.

6.6. VARIANCE OF ENERGY OF MOVING SUBTRACTION AND ITS RANGES

Given an energy of moving subtraction, K, of an m x n motif $M^s=[f^s(c, d)]$ and the circular shift motifs M_{ij}^r of another motif $M^r = [f^r(c, d)]$ and their 1-norm metrics, $\left\{u_{11}^{s,r}, u_{12}^{s,r}, ..., u_{mn}^{s,r}\right\}$, the variance of energy is defined as $V_{s,r} = \sum_{i=1}^{m}\sum_{j=1}^{n}\left(K_{s,r} - u_{ij}^{s,r}\right)^2 / N$ where $N = m \,.\, n$, $1 \le c, i \le m$ and $1 \le d, j \le n$. Given any m x n defect-free motif(s) and defective motif(s) in lattice L,

- Let $\overline{V}_{s,r}$ be the variance of energies between defect-free motifs and defective motif(s), then $_{Vs,r} - \Phi \le \overline{V}_{s,r} \le V_{s,r} + \Phi$, where $\Phi = 2(mn\, K_{s,r} + 1)\, |e| + |e|^2$, the energy of moving subtraction, $K_{s,r}$ and the defect values, $e \in R$.
- For all $e \ne 0$, there exists a tolerance $\gamma \ge 0$ such that the difference in variance of energies between defect-free motifs and defective motif(s) is $0 \le \gamma \le |\overline{V}_{s,r} - V_{s,r}| \le \Phi$, where some $\Phi \in R$.

The 2D plane of the variance of energy (V) versus the energy of moving subtraction (E) is called an E-V space for convenience.

6.7. FORMULATION OF DECISION BOUNDARIES

Given any m × n defect-free motif in lattice L=[f(c,d)], with variance of energies of the defect-free motifs and its energies given as $V_{s,r}$ and $K_{s,r}$, respectively. Since there exist two tolerances in the difference of energies between

$K_{s,r}$ and $\overline{K}_{s,r}$ and variances of energies between, $V_{s,r}$ and $\overline{V}_{s,r}$, for defect-free motifs and defective motif(s), namely,

(a) $0 \le \delta \le |\overline{K}_{s,r} - K_{s,r}| \le m \,.\, n \,.\, |e|$ and

(b) $0 \le \gamma \le |\overline{V}_{s,r} - V_{s,r}| \le \Phi$.

They form four boundaries defining a defect-free region. In other words, ($K_{s,r}$, $V_{s,r}$) can form a coordinate point on the x-y plane where defective motif(s), the energies $\overline{K}_{s,r}$ and variances of energies, $\overline{V}_{s,r}$, could be in one of the following regions

(1) $K_{s,r} - mn \,.\, |e| \le K_{s,r} < K_{s,r} - \delta$, (or)

(2) $K_{s,r} + \delta < \overline{K}_{s,r} \le K_{s,r} + mn \,.\, |e|$, (or)

(3) $V_{s,r} - \Phi \le \overline{V}_{s,r} < V_{s,r} - \gamma$, (or)

(4) $V_{s,r} + \gamma < \overline{V}_{s,r} \le V_{s,r} + \Phi$, (or)

where $\delta \ge 0$, $\gamma \ge 0$, $\Phi = 2(mn\, K_{s,r} + 1)\, |e| + |e|^2$, $|e| = |e^{s,r}|$, $e^{s,r} \in R$.

This is further interpreted as an E-V plot of a set of defect-free samples, with the four boundaries drawn horizontally and vertically and arrows pointing into the bounded region for the defect-free case. An example is shown in Figure 6.4a and 6.4b which depicts the E-V plot for some defect-free and defective lattices. It can be clearly seen from the plot that E-V values of the defective lattices fall significantly outside the boundaries, indicating the presence of defects. It should also be noted that some of the points, although not many, fall within the boundaries. However, this does not alter the conclusion.

In summary, the proposed methodology consists of eight major steps. The lattices and motifs are to be extracted using an automated process. Next two steps calculate the energy and variance, respectively. During this calculation both circular shift operations and spatial relationships are considered. Given the two sets of values for a given defect-free lattice and a number of training lattices, the next determines the decision boundaries from the E-V plot. Once the boundaries

are determined, the proposed methodology discerns defective lattices from defect-free lattices. In addition, the E-V points that fall outside the boundaries indicate which motif is being defective.

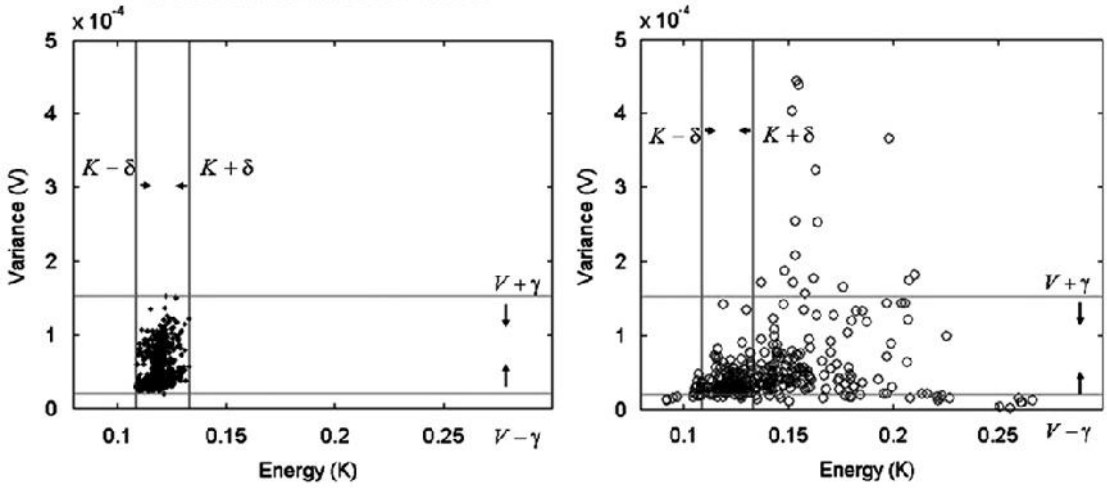

Figure 6.4 : Boundaries and E-V Plot of (a) Defect-free Lattices and (b) Defective Lattices

This chapter presented the motif based algorithm for detecting defects from patterned fabrics. The method exploited lattices and motifs properties for defect detection. The study, thus proposes enhancement algorithm to improve the quality of the input patterned fabric, 13 non-motif-based algorithms and one motif-based algorithm for detecting defects in patterned fabric. Several experiments were conducted to evaluate the performance of these proposed techniques. The results of the experiments are presented and discussed in the next chapter, Results and Discussion.